

Anisotropic Packing and One-Dimensional Fluctuations of C_{60} Molecules in Carbon Nanotubes

K. H. Michel,¹ B. Verberck,¹ and A. V. Nikolaev²

¹*Department of Physics, University of Antwerp, Groenenborgerlaan 171, 2020 Antwerp, Belgium*

²*Institute of Physical Chemistry of the Russian Academy of Sciences, Leninskii prospekt 31, 117915 Moscow, Russia*

(Received 1 June 2005; published 28 October 2005)

The confinement of a C_{60} molecule encapsulated in a cylindrical nanotube depends on the tube radius. In small tubes with radius $R_T \lesssim 7 \text{ \AA}$, a fivefold axis of the molecule coincides with the tube axis. The interaction between C_{60} molecules in the nanotube is then described by a O_2 -rotor model on a 1D liquid chain with coupling between orientational and displacive correlations. This coupling leads to chain contraction. The structure factor of the 1D liquid is derived. In tubes with a larger radius the molecular centers of mass are displaced off the tube axis. The distinction of two groups of peapods with on- and off-axis molecules suggests an explanation of the apparent splitting of A_g modes of C_{60} in nanotubes measured by resonant Raman scattering.

DOI: 10.1103/PhysRevLett.95.185506

PACS numbers: 61.48.+c

The synthesis [1] of self-assembled chains of C_{60} molecules inside single-walled carbon nanotubes (SWCNTs), peapods $(C_{60})_N@SWCNT$, has opened the road for the study of a unique class of nanoscopic hybrid materials with unusual electronic [2] and structural properties. Electron microscopy observations on sparsely filled tubes [3] demonstrate the motion of molecules along the tube axis and imply that the interaction between C_{60} and the surrounding tube is due to weak van der Waals forces. By now it is possible to prepare peapods with high filling rate of C_{60} or other fullerene molecules, thereby obtaining 1D molecular chains [4] inside the tube. A prototype of a 1D chain without long-range order is the salt $Hg_{3-\delta}AsF_6$, where chains of Hg cations are intercalated into channels formed by the three-dimensional lattice of AsF_6^- [5,6]. Similarly, in the 1D conductor tetraphenyldithiapyranylidene iodide an organic matrix separates parallel channels filled with I_3^- anions [7]. In both compounds coupling between chains develops at $T_c = 120$ and 180 K, respectively, leading to a 3D ordered state. On the other hand, we expect that peapods $(C_{60})_N@SWCNT$ will behave as 1D molecular liquids down to much lower temperature (T). We have formulated a theory which takes into account the confinement of the C_{60} molecules by the nanotube wall and the displacive and orientational interactions between molecules. Although long-range order is absent, displacive and orientational correlations between C_{60} molecules lead to 1D crystal-like behavior in small tubes. In larger tubes (radius $R_T \gtrsim 7 \text{ \AA}$) the 1D character is lost. The theory suggests an explanation for resonance Raman results on C_{60} in SWCNT and makes further predictions to be tested by experiments.

We start from one C_{60} molecule with its center of mass on the axis of an infinitely long tube. The tube is taken as a cylinder with radius R_T , its wall is approximated by a smooth surface density σ of carbon atoms (for graphite, $\sigma = 0.38 \text{ \AA}^{-2}$). The axis of the tube coincides with the Z axis of a space-fixed Cartesian system (X, Y, Z) . We consider a molecular-fixed system of axes (x, y, z) such that

these axes coincide with twofold axes of the molecule. When both systems coincide, the molecule is in standard orientation [8]. With the center of the molecule as origin, a point located at $\vec{\rho}$ on the tube has the cylindrical coordinates (R_T, Φ, Z) . The molecule (symmetry I_h) is taken as a skeleton of interaction centers (ICs) located at positions $\{\vec{r}_{\Lambda_i}\}$ on a sphere with radius $d = 3.55 \text{ \AA}$. The centers, labeled by composite indices Λ_i , are of three types: 60 atomic ICs ($i = 1$), a set of 3 ICs on each of the 30 double bonds ($i = 2$), and 60 single bond ($i = 3$) ICs [9]. They interact with the C-surface density of the tube wall by repulsive Born-Mayer and attractive van der Waals forces. The strength of the interaction potentials $u^i(r)$ is similar to the ones used for interactions between molecules in solid C_{60} [10]. Total-energy electronic structure calculations [11] show that the interaction of the C_{60} molecule with the tube is not due to chemical bonds.

The total interaction potential of the molecule with the nanotube, called nanotube field potential, reads

$$V(R_T) = \sigma R_T \sum_{i, \Lambda_i} \int_0^{2\pi} d\Phi \int_{-\infty}^{+\infty} dZ u^i(|\vec{\rho} - \vec{r}_{\Lambda_i}|). \quad (1)$$

Here, \sum_{Λ_i} stand for summations over ICs: $\Lambda_1 = 1, \dots, 60$ (atoms), $\Lambda_2 = 1, \dots, 90$ (double bond ICs), and $\Lambda_3 = 1, \dots, 60$ (single bond ICs). For an arbitrary orientation of the molecule, the positions \vec{r}_{Λ_i} of the centers depend on the Euler angles (α, β, γ) which specify the orientation of the molecule with respect to the space-fixed system. The appropriate variables (order parameters) to describe the statics and dynamics of orientationally disordered molecular crystals are molecule and site symmetry adapted rotator functions (SARFs) [12]. Here we construct cylindrical SARFs

$$U_l(\beta, \gamma) = \sum_{n=-l}^l \alpha_l^{n(I_h)} D_{n,0}^l(\beta, \gamma). \quad (2)$$

They are linear combinations of Wigner's functions

$D_{n,m}^l(\alpha, \beta, \gamma)$ with cylindrical symmetry implying $m = 0$ in Eq. (2). Molecular symmetry is reflected in the structure factors $\alpha_l^{n(I_h)}$, $l = 0, 6, 10$, with n even $\leq l$ [9]. Expanding the potential in terms of SARFs, we get

$$V(R_T; \beta, \gamma) = \sum_{l=0,6,10,\dots} v_l(R_T) U_l(\beta, \gamma), \quad (3)$$

with coefficients

$$v_l(R_T) = \sum_{i=1}^3 v^i(R_T) g_l^i, \quad (4)$$

where g_l^i are molecular shape factors accounting for the icosahedral distribution of ICs of each type [9]. Although it is possible to evaluate Eq. (1) directly by performing the required coordinate transformations (Euler rotations) followed by numerical integration, the formulation in terms of SARFs is necessary for the evaluation of scattering laws and thermal expectation values [9]. A practical advantage of Eq. (3) is its rapid convergence: a restriction to terms $l \leq 12$ considerably reduces the computation time for a (β, γ) plot of $V(R_T; \beta, \gamma)$.

For a fixed set of interaction potential parameters, we have plotted the potential $V(R_T; \beta, \gamma)$, for different tube radii, in form of Mercator [13] maps as a function of the angles $0 \leq \beta \leq \pi$ and $0 \leq \gamma \leq 2\pi$. Figure 1 with $R_T = 6.86 \text{ \AA}$ corresponds to $n = 10$ for (n, n) armchair tubes. Twelve equivalent potential minima—which determine the most probable orientation of the molecule—are found. The values $(\beta \approx 58^\circ, \gamma = 0)$ correspond to the situation where the molecule is rotated counterclockwise around the Y axis, away from the standard orientation by an angle $\beta = \arccos 2/(10 + 2\sqrt{5})^{1/2}$. Then, the nanotube's long axis intersects the centers of two opposing pentagons (a fivefold axis of C_{60} coincides with the tube axis). The minima in Fig. 1 correspond to the 12 pentagons on the C_{60} molecule. The 20 maxima correspond to the energetically unfavorable orientation when the tube axis intersects two opposing hexagon faces (a threefold axis of C_{60} coincides with the tube axis). Increasing the nanotube radius but leaving the center of mass of the molecule on the tube axis, we find that

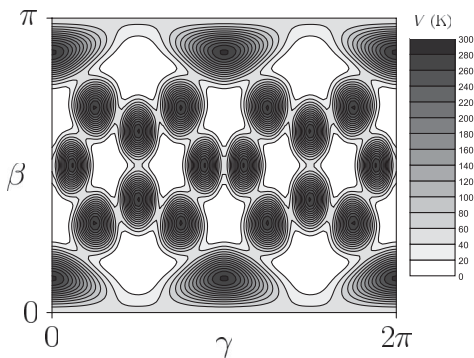


FIG. 1. Mercator map of nanotube field potential $V(R_T; \beta, \gamma)$, units K, $R_T = 6.86 \text{ \AA}$. Energy measured from its minimum.

the Mercator maps change. For the $(12, 12)$ tube with $R_T = 8.24 \text{ \AA}$ and for tubes with larger radii, we obtain a plot where in comparison with Fig. 1 the positions of the maxima and the minima are exchanged, a threefold axis of the C_{60} molecule coincides with the tube axis. In the range $7 \text{ \AA} \leq R_T \leq 8 \text{ \AA}$, we find an intermediate situation where a twofold axis of the molecule coincides with the tube axis. This orientation favors polymerization of C_{60} molecules [14]. However, more important than the change of molecular orientation is the fact that, with increasing radius the nanotube axis is no longer a locus of stability for the center of mass of the molecule. In Fig. 2, we have plotted the interaction potential $V(R_T; \Delta)$ of the C_{60} molecule with a fivefold axis parallel to the tube axis as a function of the distance Δ of the center of mass of the molecule from the tube axis. For the $(11, 11)$ tube, $R_T = 7.55 \text{ \AA}$, the potential difference between the maximum on axis and the minimum off axis at $\Delta_m = 1.1 \text{ \AA}$ is $\approx 5 \times 10^3 \text{ K}$ and an order of magnitude larger than any effect of molecular orientation. The displacement of the molecular center-of-mass position away from the nanotube axis for larger tubes reflects the increasing importance of the attractive parts of the van der Waals potential at the expense of the repulsive parts. For $C_{60}@ (12, 12)$ we obtain $\Delta_m = 1.8 \text{ \AA}$, comparable to 1.6 \AA from first-principles calculations [15]. Our results of Fig. 2 are in qualitative agreement with potential energy calculations where a homogeneous distribution of C atoms on both the C_{60} molecule and the nanotube was assumed [16]. The large energy differences (order eV) between minima of $V(R_T)$ for $R_T \leq 7 \text{ \AA}$, $\Delta_m = 0$ and $R_T \geq 7 \text{ \AA}$, $\Delta_m \neq 0$, respectively, suggests a classification of $C_{60}@SWCNT$ peapods into two groups depending on the tube radius: small nanotubes with molecular center-of-mass positions on axis and larger tubes, with off-axis positions.

Resonance Raman scattering [17] measurements on single-walled carbon nanotubes filled with C_{60} molecules exhibit an unexpected splitting of the totally symmetric modes of the C_{60} molecule. In particular, the pentagonal

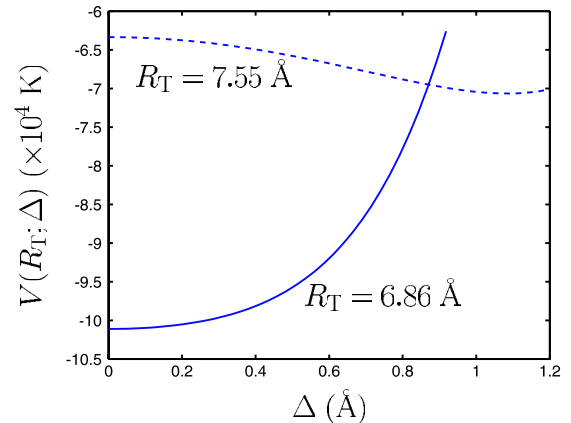


FIG. 2 (color online). Variation of nanotube field potential with Δ .

pinch mode $A_g(2)$ “splits” into a doublet $A_g(2)'$ and $A_g(2)''$ below room temperature. This mode, located at 1469 cm^{-1} in pristine C_{60} , can be used as a probe for structural and electronic properties. We attribute the observed splitting of the A_g modes of the C_{60} molecule to two distinct symmetry breakings of the molecule resulting from the on- and off-axis center-of-mass position for small and large nanotubes, respectively. Experiments are carried out on C_{60} @SWCNT with a dispersion of tube radii. This resolves the paradox that there should be no splitting for the nondegenerate A_g modes. The present explanation is corroborated by the experimental fact [17] that thinner tubes tend to yield stronger $A_g(2)''$ components. From Fig. 2 we see that the nanotube field is larger in absolute value for the smaller than for the larger peapods at their respective molecular center-of-mass positions Δ_m .

While in C_{60} peapods, the dependence of the nanotube field on molecular orientations leads only to weak energy differences, it should be more important for more anisotropic molecules such as C_{70} . There a splitting of electron diffraction peaks is interpreted in terms of two distinct orientations of the C_{70} molecule [4]. We expect that the corresponding distinct nanotube fields will also lead to a splitting of A' Raman peaks.

From Fig. 2 we conclude that the stable center-of-mass positions of the C_{60} molecules inside the (10, 10) nanotube are located on the tube axis and hence form a 1D chain. The 1D character of a system of structureless C_{60} molecules inside a (10, 10) nanotube has been confirmed by Monte Carlo simulations [16]. In the following, we study by analytical methods a 1D model of $(C_{60})_N$ @SWCNT with small tube radii, i.e., with a fivefold axis of each molecule in coincidence with the tube axis. Starting from a model potential [9,10] between two C_{60} molecules, we formulate the interaction potential of a chain of N molecules inside the nanotube by performing a double expansion in displacive and angular variables. Minimizing the zeroth-order term of the expansion in angular coordinates with respect to displacements along the tube axis, we find the average center-of-mass distance $a = 10.211\text{ \AA}$. The next-order term is transformed into a O_2 -symmetry rotor model:

$$V^{\text{RR}} = \sum_{n=2}^N J \vec{S}(n) \cdot \vec{S}(n-1), \quad (5)$$

where the rotational coordinate reads

$$\vec{S}(n) = (\cos[5\psi(n)], \sin[5\psi(n)]), \quad (6)$$

$\psi(n)$ being the rotation angle of the n th molecule about the tube axis (Z) measured away from the X axis. The quantity J stands for the rotational energy coupling between two neighboring molecules at distance a . We find that $J < 0$, the rotational interaction between neighboring molecules is attractive and maximum if both molecules have the same orientation angle ψ . Since C_{60} has a center of inversion symmetry, the same orientation of two nearest-neighbor

molecules implies that their neighboring faces are in staggered orientation.

Within the rotor model, orientational correlations between distant molecules are given by thermal averages:

$$\Gamma(r) = \langle \vec{S}(n) \cdot \vec{S}(n+r) \rangle = (\Gamma(1))^r, \quad (7)$$

where r is an integer and $\Gamma(1) = \langle \vec{S}(n) \cdot \vec{S}(n-1) \rangle = I_1(j)/I_0(j)$ is the nearest-neighbor correlation [18]. Here $j = |J|/T$ and I_1, I_0 are modified Bessel functions. For finite T , $\Gamma(1) < 1$, and $\Gamma(r)$ tends to zero with increasing r ; i.e., there is no long-range orientational order. At $T = 0$, $\Gamma(1) = 1$, and perfect order appears.

We add translational (T) degrees of freedom of the chain in form of an harmonic interaction potential

$$V^{\text{TT}} = \frac{f}{2} \sum_n [\zeta(n) - \zeta(n-1) - a]^2. \quad (8)$$

Here $\zeta(n)$ stands for the center-of-mass position of the n th molecule on the Z axis of the tube and a is the average separation between two neighboring molecules. The average spring constant f is obtained from the second derivative of the intermolecular van der Waals interaction with respect to the displacements. A harmonic interaction potential has been introduced previously [19] for an individual chain of Hg ions in $\text{Hg}_{3-\delta}\text{AsF}_6$. The mean square deviation in the relative positions of neighboring molecules reads $\langle [\zeta(n) - \zeta(n-1) - a]^2 \rangle = \sigma^2 = T/f$.

The coupling of orientational and translational degrees of freedom is obtained in the form

$$V^{\text{RRT}} = \lambda \sum_n \vec{S}(n) \cdot \vec{S}(n-1) [\zeta(n) - \zeta(n-1) - a], \quad (9)$$

where $\lambda > 0$ is the rotation-rotation translation (RRT) coupling derived from the intermolecular potential. In solid C_{60} , the V^{RRT} coupling [20] leads to a contraction of the cubic lattice at the structural phase transition. In the present case the lattice contraction is obtained as

$$\langle \zeta(n) - \zeta(n-1) - a \rangle = -\lambda \Gamma(1)/f. \quad (10)$$

We find $J = -19\text{ K}$, $\lambda = 79\text{ K \AA}^{-1}$, and $f = 18255\text{ K \AA}^{-2}$, implying a room-temperature contraction of $-\lambda \Gamma(1)/f = -0.00014\text{ \AA}$. The interaction V^{RRT} is reminiscent of the spin-lattice interaction in compressible magnets [21].

Since in the 1D model the second moment $\langle \zeta^2(n) \rangle$ diverges, there is no long-range crystalline order. The vanishing of the Debye-Waller factor implies that there are no ideal Bragg peaks. We apply concepts introduced for the description of $\text{Hg}_{3-\delta}\text{AsF}_6$ [6,19] and show that the structure factor has characteristic resonances in reciprocal space. The static structure factor of the center-of-mass positions of the 1D chain is given by

$$S(q) = \frac{1}{N} \sum_{n,n'} \langle e^{iq[\zeta(n) - \zeta(n')]} \rangle, \quad (11)$$

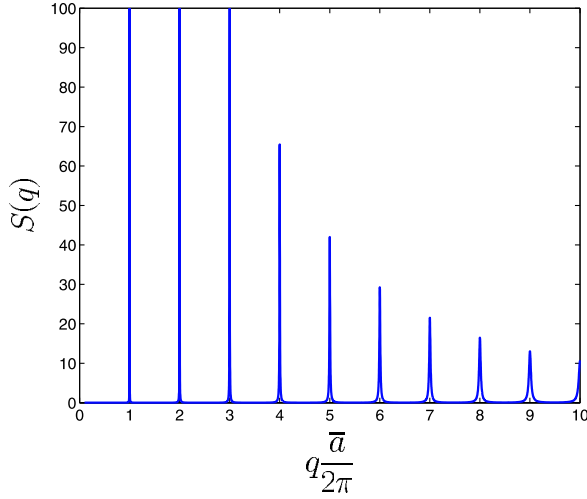


FIG. 3 (color online). Structure factor $S(q)$, given by Eq. (12), for $T = 300$ K. For $q \frac{\bar{a}}{2\pi} \in \mathbb{Z}_0$, $S(q)$ reaches local maxima $\frac{1+Z(q)}{1-Z(q)}$.

where the brackets denote a thermal average and where q is the wave vector transfer in Z direction. Taking into account the interaction potentials V^{TT} and V^{RRT} and retaining short-range correlations, we find

$$S(q) = \frac{1 - Z^2(q)}{1 + Z^2(q) - 2Z(q) \cos(q[a - \lambda\Gamma(1)/f])}, \quad (12)$$

where $Z(q) = \exp(-q^2\sigma^2/2)$ with $\sigma^2 = T/f$. This expression of $S(q)$ is an extension of previous results [6,19] where only the displacive potential V^{TT} was considered. Now, in the argument of the cosine function in Eq. (12), the average lattice spacing a between molecules without orientational correlations is replaced by the shorter length $\bar{a} = a - \lambda\Gamma(1)/f$, which includes orientational correlations and decreases with decreasing T . In Fig. 3 we have plotted $S(q)$ for $T = 300$ K. The function $S(q)$ exhibits narrow peaks which appear as streaks in the experimental diffraction pattern [4].

We have shown that the chain of C_{60} molecules in SWCNT is a physical realization of the O_2 -rotor model. The rotational interaction V^{RR} and the coupling V^{RRT} between rotational and translational motion should be relevant for the theoretical explanation of inelastic neutron scattering experiments [22] on the dynamics of C_{60} molecules inside SWCNTs. The present analytical methods and results can be extended to the study of C_{60} encapsulated in boron-nitride nanotubes [14,23].

The authors thank P. Launois and D. Lamoen for useful discussions. The present work has been supported by the Bijzonder Onderzoeksfonds, Universiteit Antwerpen (BOF—NOI).

- [1] B.W. Smith, M. Monthieux, and D.E. Luzzi, *Nature (London)* **396**, 323 (1998).
- [2] D.J. Hornbaker, S.J. Kahnq, S. Misra, B.W. Smith, A.T. Johnson, E.J. Mele, D.E. Luzzi, and A. Yazdani, *Science* **295**, 828 (2002).
- [3] B.W. Smith, M. Monthieux, and D.E. Luzzi, *Chem. Phys. Lett.* **315**, 31 (1999).
- [4] K. Hirahara, S. Bandow, K. Suenaga, H. Kato, T. Okazaki, H. Shinohara, and S. Iijima, *Phys. Rev. B* **64**, 115420 (2001).
- [5] I.D. Brown, B.D. Cutforth, C.G. Davies, R.J. Gillespi, P.R. Ireland, and J.E. Vekris, *Can. J. Chem.* **52**, 791 (1974).
- [6] R. Spal, C.E. Chen, T. Egami, P.J. Nigrey, and A.J. Heeger, *Phys. Rev. B* **21**, 3110 (1980); for a review, see P.M. Chaikin and T.C. Lubensky, *Principles of Condensed Matter Physics* (Cambridge University Press, Cambridge, 1995), Chap. 6.
- [7] P.A. Albouy, J.P. Pouget, and H. Strzelecka, *Phys. Rev. B* **35**, 173 (1987).
- [8] W.I.F. David, R.M. Ibberson, J.C. Matthewman, K. Prassides, T.J.S. Dennis, J.P. Hare, H.W. Kroto, R. Taylor, and D.R.M. Walton, *Nature (London)* **353**, 147 (1991).
- [9] J.R.D. Copley and K.H. Michel, *J. Phys. Condens. Matter* **5**, 4353 (1993); D. Lamoen and K.H. Michel, *Z. Phys. B* **92**, 323 (1993).
- [10] In the notation of Ref. [9], $C_1^{\text{aa}} = 3.24 \times 10^7$ K, $C_2^{\text{aa}} = C_2^{\text{as}} = C_2^{\text{ss}} = 3.6 \text{ \AA}^{-1}$, $B^{\text{aa}} = 4.58 \times 10^5 \text{ K \AA}^6$, $C_1^{\text{as}} = 3C_1^{\text{ad}} = 6.33 \times 10^6$ K, $C_2^{\text{ad}} = 3.4 \text{ \AA}^{-1}$, $C_1^{\text{dd}} = 1.1 \times 10^6$ K, $C_1^{\text{ss}} = 5.92 \times 10^6$ K, $C_2^{\text{dd}} = 3.2 \text{ \AA}^{-1}$, and others are zero.
- [11] S. Okada, S. Saito, and A. Oshiyama, *Phys. Rev. Lett.* **86**, 3835 (2001).
- [12] H.M. James and T.A. Keenan, *J. Chem. Phys.* **31**, 12 (1959).
- [13] Gerardus Mercator (1512–1594), Flemish cartographer, inventor of the cylindrical projection.
- [14] A. Trave, F.J. Ribeiro, S.G. Louie, and M.L. Cohen, *Phys. Rev. B* **70**, 205418 (2004).
- [15] S. Okada, M. Otani, and A. Oshiyama, *Phys. Rev. B* **67**, 205411 (2003).
- [16] M. Hodak and L.A. Girifalco, *Phys. Rev. B* **68**, 085405 (2003).
- [17] R. Pfeiffer, H. Kuzmany, T. Pichler, H. Kataura, Y. Achiba, M. Melle-Franco, and F. Zerbetto, *Phys. Rev. B* **69**, 035404 (2004).
- [18] H.E. Stanley, *Phase Transitions and Critical Phenomena* (Clarendon, Oxford, 1971).
- [19] V.J. Emery and J.D. Axe, *Phys. Rev. Lett.* **40**, 1507 (1978).
- [20] D. Lamoen and K.H. Michel, *Phys. Rev. B* **48**, 807 (1993).
- [21] H. Wagner, *Phys. Rev. Lett.* **25**, 31 (1970).
- [22] J. Cambedouzou, S. Rols, R. Almairac, J.L. Sauvajol, H. Kataura, and H. Schober, *Phys. Rev. B* **71**, 041403(R) (2005).
- [23] W. Mickelson, S. Aloni, W.Q. Han, J. Cummings, and A. Zettl, *Science* **300**, 467 (2003).